Supporting Information

Rostovtseva *et al.* 10.1073/pnas.0806303105

SI Materials and Methods

Protein Purification. Frozen rat brains were thawed, homogenized in assembly buffer [0.1 M Mes, 1 mM EGTA, 1 mM $MgCl_2$ (pH 6.9)], and centrifuged at 100,000 × *g*. Microtubule protein (tubulin plus microtubule-associated proteins) was purified by several rounds of GTP-driven, temperature-dependent polymerization and depolymerization (1). Tubulin was then purified from this material by selective polymerization in high-buffer concentration, pelleted by centrifugation, redissolved in assembly buffer at 25 mg/mL, and drop-frozen in liquid nitrogen as in ref. 2. Tubulin from *Leishmania tarentolae* was purified as described in ref. 3 and was a kind gift from K. Werbovetz (Ohio State University, Columbus, OH).

Single-Channel Current Analyses. Current measurements were performed by using an Axopatch 200B amplifier (Axon Instruments) in the voltage-clamp mode. Data were filtered by a low-pass 8-pole Butterworth filter (model 9002; Frequency Devices) at 15 kHz and saved directly into the computer memory with a sampling frequency of 50 kHz as described in ref. 4. For data analysis, a digital 8-pole Bessel low-pass filter set at 500 Hz was applied to all records, and then individual events of current blockages were discriminated. Lifetimes were calculated by fitting logarithmic single or double exponentials to logarithmically binned histograms of at least 200 blockage events (5). Nine different logarithmic probability fits were generated with different fitting procedures, and the mean ± SD of the fitted time constants was used as mean ± SD for the lifetime.

The voltage-dependent properties of the voltage-dependent anion channel (VDAC)-containing membrane were assessed by applying a symmetrical 5-mHz triangular voltage wave with ±60 mV amplitude from a Function Waveform Generator Hewlett–Packard 33120A and recording the current by using a Digidata 1322A (Axon Instruments). Data acquisition and analysis were done as described in ref. 4.

Mitochondria Isolation. Male Wistar rats (250–300 g) were used throughout the study. Brain mitochondria were isolated from the forebrains as described in ref. 6. Cardiac mitochondria were isolated from rat hearts by a method described in ref. 7 by using successive treatments of heart tissue homogenates by trypsin and trypsin inhibitor. The final mitochondrial pellet was suspended in 2 mL of Mitomed solution [0.5 mM EGTA, 3 mM $MgCl_2$, 60 mM potassium lactobinate, 20 mM taurine, 3 mM KH_2PO_4, 20 mM Hepes, 110 mM sucrose, 0.5 mM DTT (pH 7.1)].

1. Sackett DL, Knipling L, Wolff J (1991) *Protein Expr Purif* 2:390–393.
2. Wolff J, Sackett DL, Knipling L (1996) Cation selective promotion of tubulin polymerization by alkali metal chlorides. *Protein Sci* 5:2020–2028.
3. Yakovich AJ, Ragone FL, Alfonzo JD, Sackett DL, Werbovetz KA (2006) *Exp Parasitol* 114:289–296.
4. Rostovtseva TK, Kazemi N, Weinrich M, Bezrukov SM (2006) Voltage gating of VDAC is regulated by nonlamellar lipids. *J Biol Chem* 281:37496–37506.
5. Sigworth FJ, Sine SM (1987) *Biophys J* 52:1047–1054.
6. Booth RF, Clark JB (1978) A rapid method for the preparation of relatively pure metabolically competent synaptosomes from rat brain. *Biochem J* 176:365–370.
7. Saks VA, Chernousova GB, Gukovsky DE, Smirnov VN, Chazov EI (1975) *Eur J Biochem* 57:273–290.

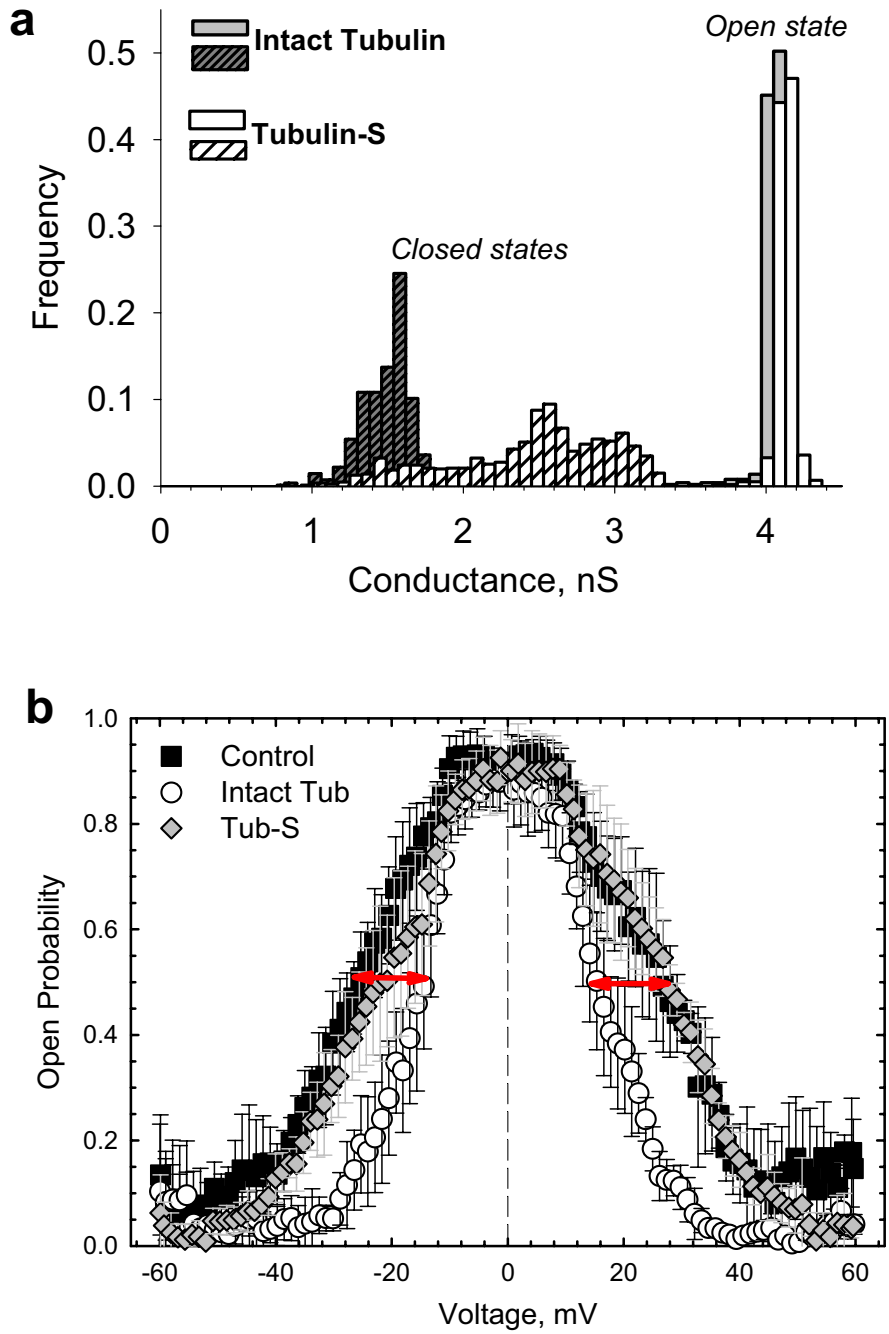

Fig. S1. Tubulin-S does not induce VDAC closure characteristic to intact tubulin. (*a*) Tubulin-S induces a broader distribution of closed states than intact tubulin. Distributions of the open- and closed-state conductance were obtained in the presence of 50 nM intact tubulin and tubulin-S. The applied voltage was −25 mV. Experimental conditions were as in Fig. 3 *A* and *C*. (*b*) Tubulin increases VDAC propensity to close, whereas tubulin-S is not distinguishable from control. To test the effect of tubulin C-terminal tail (CTT) on multichannel membranes and on VDAC voltage-gating parameters, the probability of VDAC channels to be open or closed at different potentials in the presence of intact tubulin and tubulin-S was analyzed. As was anticipated from the single-channel experiments, tubulin increased voltage gating, which is seen as a shift of the bell-shaped voltage dependence toward the smaller voltages. Open probability is defined as the ratio $(G - G_{min})/(G_{max} - G_{min})$, where G_{max} and G_{min} are the maximum and minimum conductances, respectively. Only part of the wave during which the channels were reopening was used for the subsequent analysis. Data were collected as described in ref. 4 and are means of 4–7 independent experiments ±SE on membranes containing 10–50 channels. Fifty nanomolar intact tubulin or tubulin-S was added to the both sides of the membrane. Experimental conditions were as in Fig. 3 *A* and *C*.

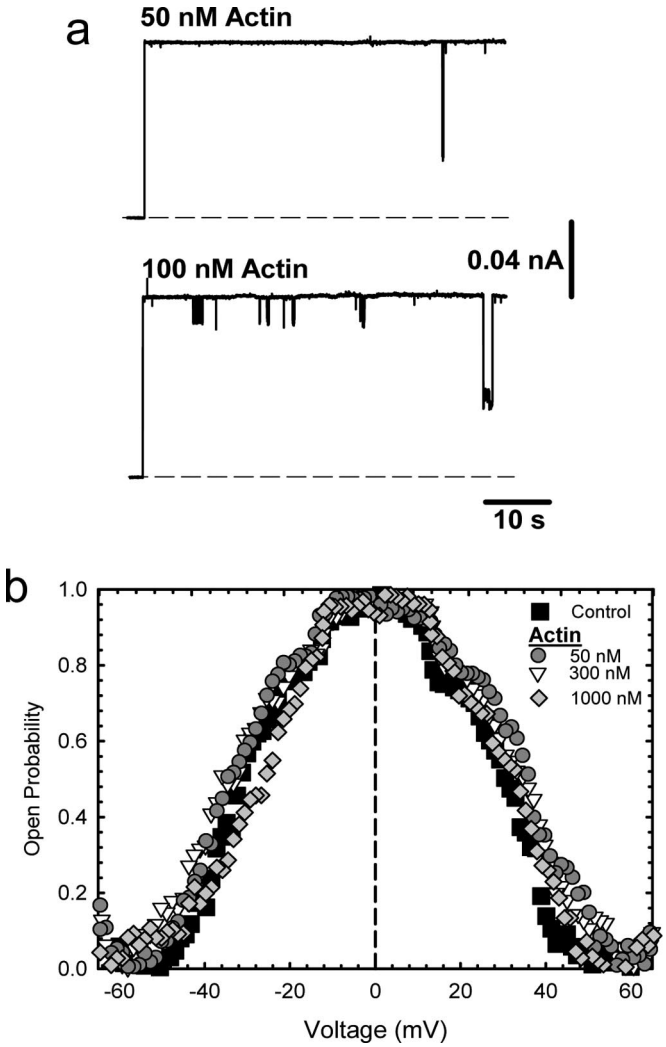

Fig. S2. Actin does not block VDAC channel or change VDAC gating parameters. (*a*) Actin (50 or 100 nM) added to the *cis* side of the membrane does not block channel conductance. Current traces through the single VDAC channel were obtained at −25 mV applied potential. Experimental conditions were as in Fig. 3*A*. (*b*) Actin (50, 300, or 1,000 nM) added to both sides of the membrane containing 30 channels does not affect VDAC gating. Open probability is defined as in Fig. S1*b*. The medium consisted of 1 M KCl, buffered with 5 mM Hepes at pH 7.4. VDAC was isolated from *Neurospora crassa* mitochondria. Bilayer membranes were formed from asolectin with 10% cholesterol.

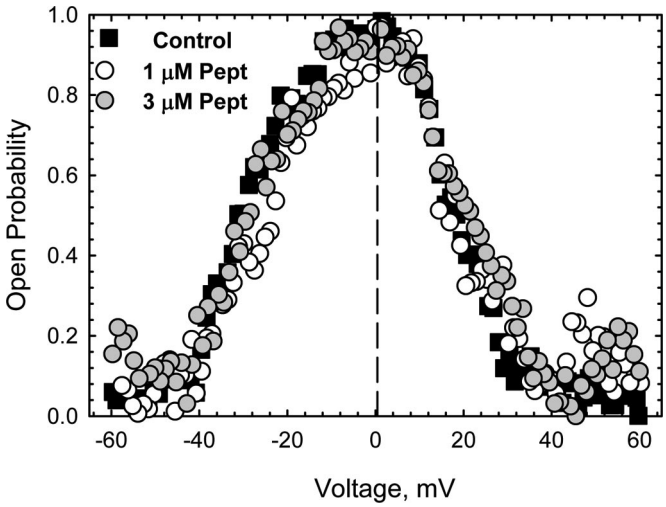

Fig. S3. VDAC voltage gating is not affected by CTT synthetic peptides. Mixtures of 1 and 3 μM α- and β-tubulin CTT synthetic peptides were added to both sides of the membrane. Experimental conditions were as in Fig. 3*B*.

a

Species	Accession	Sequence
Eukaryotes with mitochondria		
Homo sapiens (Kα-1)	NM_006082	VGVDSV EGEGEEEGEEY
Gallus gallus	CAA30852	VGLDSY EDEEEGEE
" (a2)	XM_419249	VGTDSM DGEDEGEEY
" (a8)	NM_205444	VATDLF EDENEAGES
Danio rerio	AAB84143	VGAESV EGEDEGEEY
Notophthalmus viridescens	Q91060	VGLDSY EGEEDEGEEY
Xenopus laevis	P08537	VGADSA DAEDEGEEY
Brugia malyi	XP_001899189	VGIDSL EGEGEGEEY
Drosophila melanogaster (a85E)	NM_079573	VGIDST TELGEDEEY
" (a67C)	NM_079285	VGLDNA EEGGDEDFDEF
Homarus americanus	Q94570	VGIDTA DGEDDEEANDY
Aplysia californican	Q8T6A5	VGVDSV DAEGEDEGEEY
Arabidopsis thaliana	NM_121983	VGAEGG DDEEDEGEDY
Triticum aestivum	P14640	VGAEFD EGEDGDEGDEY
Zea mays	P22275	VAAEGG SDDGDEEEEY
Leishmania tarentolae	ABC40566	VGAESA DDMGEEDVEEY
Toxoplasma gondii	P10873	VGIETA EGEGEEEGYGDEY
Blepharisma japonicum	Q08629	VGIETA EAEGEEEGYGEEL
Tetrahymena thermonphila	AAA21350	VGIETA EGEGEEGY
Saccharomyces cerevisiae	NP_013625	VGADSY AEEEEF
Schizosaccharomyces pombe	CAA16866	VGGDSM DNEMYEADEEY
Neurospora crassa	P38668	VAGDYN DVDVDAEY
Schizophyllum commune	CAA60035	VGTDSA DAEEEGEY
Dictyostelium discoidium	P32255	VSASTE GEEQEEEY
Pelvetia fastigiata	Q40831	VGAETA GDGEEEEFGEEY
Euglena gracilis	P33625	VGAESA DVEGEEDVEEY

Fig. S4. Sequence alignment of tubulin CTT from various species. The species name and accession number are given for each sequence, followed by the sequence. All sequences are aligned by using the C terminus of the final helix in the crystal structure; these residues begin each sequence line. The space in each line indicates the end of the residues resolved in the crystal structure and the beginning of the CTT. The structures used were Protein Data Base (PDB) ID code 1JFF for all eukaryotic tubulins and PDB ID code 2BTQ for the bacterial tubulins. α-Tubulin CTT sequences are in *a*, and β-tubulin CTT sequences are in *b*. Many species have multiple genes for α and β. In these cases, the sequence shown is one that is similar to the average character shown in Fig. 6*B* in the text.

Naeglaria gruberi	P11237	VGTESQ EGDGEEGEDGGDQ
Eukaryotes lacking mitochondria – near normal CTT		
Giardia lamblia	XP_001706843	IGAETL GDGEGEDMEEDDAY
Trichomonaas vaginalis	XP_001330666	VAAESV EGGDEEEDGGEM
Encephalitozoon intestinalis	AAN78301	IGAETL GDGEGEDMEEDDAY
Eukaryotes lacking mitochondria – truncated or decharged CTT		
Guillardia theta	Q9SCC8	VGSESQ DLISNSFF
Hemiselmis andersenii	XP_001712353	VGNENN EEDILEY
Encephalitozoon cuniculi	NP_586048	ISSNAE PVDEY
Entamoeba dispar	XP_001739532	LAIDNT VEGESMTAQ
Bacteria		
Prosthecobacter dejongeii (BTubA)	AAO12155	YQVAEE SGAKAKVQLSAGDTGMRAAAAGVSDDARGSMSLRDLVDRRR
" (BTubB)	AAO12159	SYRDAS
Prosthecobacter vanneervenii (BTubA)	CAJ14012	YQVAEE SGAKAKVQPSSADYPRSSASSDDSRSGMSLRDLVDRRRA
" (BTubB)	CAJ14013	SYRDAS
Prosthecobacter debontii (BTubA)	AM041149	YQVAEE SGAKAKIQDVSGETVSRSSSMDDPRSTMSLRDLVERRR
" (BTubB)	AM041149	SYRDAS

Fig. S4a. *Continued.*

b

Species	Accession	Sequence
Eukaryotes with mitochondria		
Homo sapiens	AAB59507	QQYQD ATADEQGEFEEEGEDEA
Gallus gallus (b2b)	NM_001004400	QQYQD ATADEQGEFEEEFEEDEA
" (b6)	NM_001031012	QQYQE ATANDGEEAFEDDEEEINE
Danio rerio	NP_001070241	QQYQE ATADDEADFGEEGE
Xenopus laevis	P13602	QQYQD ATADEQGEFEEEEDEA
Brugia malyi	XP_001896615	QQYQD ATADEEQDLQEGESEYIEQEE
Drosophila melanogaster (56D)	NP_523795	QQYQE ATADEDAEFEEEQEAEVDEN
" (97EF)	NP_65166	QQYQE ATADDEVEFDDEQAEQ
Homarus americanus	Q25009	QQYQE ATADDEAEFEEEGEVEGEYA
Aplysia californican	AAP13560	QQYQD ATAEDEGEFDEEEGDEGGEEYA
Arabidopsis thaliana	BAB10059	QQYQD ATADEEEGYEYEEDEVEVQEEQ
Triticum aestivum	AAD10492	QQYQD ATADEEEELYEDEDDADLQE
Zea mays	Q43695	QQYQD ATAEEYDEEEQEGEEEHD
Leishmania tarentolae	ABC40567	QQYQD ATVEEEGEYDEEEEPT
Toxoplasma gondii	P10878	QQYQD ATAEEEGEFDEEEGEMGAEEGA
Tetrahymena thermonphila	P41352	QQYQD ATAEEEGEFEEEEGEN
Saccharomyces cerevisiae	P02557	QQYQE ATVEDDEEVDENGDFGAPQNQDEPITENFE
Schizosaccharomyces pombe	P05219	QQYQE AGIDEGDEDYEIEEEKEPLEY
Neurospora crassa	XP_957669	QQYQD AQVDEEEEEYEEEAPLEGEE
Schizophyllum commune	CAA44972	QQYQD ATVEEEGEYEEEVIEDGE
Dictyostelium discoidium	P32256	QQYSN QETEEDGGEYQEEHEEHEEQAEN
Ectocarpus variabilis	AAA33284	QQYQD ATAEEEGEFDEDEELDDAMG
Euglena gracilis	P12457	QQYQD ATVEEEGEFDEEEDVEQY
Naeglaria gruberi	P34108	QQYQD ATAEEEGEFDENEGAEQEEQPALY
Eukaryotes lacking mitochondria – near normal CTT		

Fig. S4b

Entamoeba dispar	EDR29554	QQYYN TPLILDEGFEPEGLLPTEVQQEETLPTNIESV
Giardia lamblia	XP_001707388	QQYQE AGVDEGEEFEEEELFGDEYA
Trichomonaas vaginalis	L05468	EMYET AGVEEQGEGEDEEGEAAA
Eukaryotes lacking mitochondria – truncated or decharged CTT		
Guillardia theta	XP_001713469	QQYQD ATMDNIAFEDQQLY
Hemiselmis andersenii	XP_001712325	QQYQE ATADGLGYEDDDLY
Enterocytozoon bieneusi	AAB72136	QQYRD SQVGGY
Encephalitozoon cuniculi	CAD26226	QQYQD ATIEEAEIFLVN
Encephalitozoon intestinalis	AAN78301	QQYQD ATVEEAEIFLVN
Bacteria		
Prosthecobacter dejongeii (BTubA)	AAO12155	YQVAEE SGAIAIVQSSAGTTGMSAAAAGVSDAAGSMSLADLVDRRL
" (BTubB)	AAO12159	SYRDAS
Prosthecobacter vanneervenii (BTubA)	CAJ14012	YQVAEE SGAIAIVQSSAGYPISSASSDDSMSGMSLADLVDRRLA
" (BTubB)	CAJ14013	SYRDAS
Prosthecobacter debontii (BTubA)	AM041149	YQVAEE SGAIAIIQSVSGTTVSSSSSMDDPSTMSLADLVDRRL
" (BTubB)	AM041149	SYRDAS

Fig. S4b. *Continued.*

Table S1. Parameters describing VDAC gating are changed in the presence of tubulin but not tubulin-S

Tubulin	Negative V_0, mV	n at negative potentials	Positive V_0, mV	n at positive potentials
Control (7)	−24.8 ± 3.2	2.9 ± 0.4	23.8 ± 5.7	2.9 ± 0.5
Intact tubulin (4)	−13.6 ± 3.2	4.1 ± 0.4	13.5 ± 4.5	3.9 ± 0.8
Tubulin-S (5)	−25.9 ± 3.6	2.5 ± 0.8	28.4 ± 1.2	2.9 ± 1.1

The gating parameters V_0 and n were obtained from the experiments shown in SI Fig. S1*b* and calculated as described in ref. 4. In the presence of 50 nM tubulin V_0, a characteristic voltage at which half-channels are open and half-closed, was shifted by 10 mV toward smaller potentials, and the gating charge, n, increased slightly from 3 to 4. In contrast, there was no measurable effect of 50 nM tubulin-S on VDAC voltage-gating parameters. Values are means ± SE. The number of experiments is shown in parentheses.